

Received:
30 July 2015Revised:
21 January 2016Accepted:
1 February 2016<http://dx.doi.org/10.1259/bjr.20150635>

Cite this article as:

Xiao W, Lin Z, Zhang W, Li M, Wu VWC. A split-parotid delineation approach for dose optimization in volumetric modulated arc therapy for nasopharyngeal carcinoma patients with parapharyngeal space invasion and level IIa cervical lymph node involvements. *Br J Radiol* 2016; **89**: 20150635.

FULL PAPER

A split-parotid delineation approach for dose optimization in volumetric modulated arc therapy for nasopharyngeal carcinoma patients with parapharyngeal space invasion and level IIa cervical lymph node involvements

¹WEI XIAO, BMed, ¹ZHIXIONG LIN, MD, ¹WUZHE ZHANG, BSc, ¹MEI LI, MMed and ^{1,2}VINCENT WC WU, PhD

¹Cancer Hospital, Shantou University Medical College, Shantou, Guangdong, China

²Department of Health Technology and Informatics, Hong Kong Polytechnic University, Hung Hom, Kowloon, Hong Kong SAR

Address correspondence to: Dr Vincent WC Wu

E-mail: htvinwu@polyu.edu.hk

Objective: This study evaluated the potential benefit of a split-parotid delineation approach on the parotid gland in the treatment planning of patients with nasopharyngeal carcinoma (NPC).

Methods: 50 patients with NPC with parapharyngeal space (PPS) and/or level IIa cervical node involvements were divided into three groups: PPS only, level IIa cervical node only and both. Two volumetric-modulated arc therapy plans were computed. The first plan (control) was generated based on the routine treatment-planning protocol, while the second plan (test) was computed with the split-parotid delineation approach, in which a line through the anterolateral margin of the retromandibular vein was created that divided the parotid gland into anterolateral and posteromedial subsegments. For the test plan, the anterolateral subsegment was prescribed, with a dose constraint of 25 Gy in the plan optimization. Dosimetric data of the parotid gland, target volumes and selected organs at risk (OARs) were compared between the control and test plans.

Results: The mean dose to the anterolateral subsegment of the parotid gland in all three groups was kept below 25 Gy. The test plan demonstrated significantly lower mean parotid dose than the control plan in the entire gland and the anterolateral subsegment in all three groups. The difference was the greatest in Group 3.

Conclusion: The split-parotid delineation approach significantly lowered the mean dose to the anterolateral subsegment and overall gland without greatly compromising the doses to target volumes and other OARs. The effect was more obvious for both PPS and level IIa cervical node involvements than for either of them alone.

Advances in knowledge: It is the first article based on the assumption that parotid gland stem cells are situated at the anterolateral segment of the gland, and applied the split-parotid delineation approach to the parotid gland in the treatment planning of patients with NPC with PPS and level IIa cervical node involvements, so that the function of the post-radiotherapy parotid gland might be better preserved.

INTRODUCTION

In external beam radiotherapy of patients with nasopharyngeal carcinoma (NPC), the parotid gland often receives a high radiation dose owing to its relatively close proximity to the tumour, especially for patients with parapharyngeal space (PPS) or upper cervical node involvements. Because of this, long-term complications such as xerostomia, sore throat, altered taste, dental decay, changes in voice quality, impaired chewing and swallowing have been reported.¹⁻⁴ With the introduction of more advanced radiotherapy techniques such as intensity-modulated radiotherapy and volumetric arc therapy in the past two decades, the dose to the parotid glands can be reduced compared with

conventional techniques, resulting in a lower incidence of severe xerostomia and better post-treatment life quality.⁵⁻⁷ However, total sparing of the parotid gland is still not possible even with these techniques; about 40% of patients with NPC were still reported to have moderate or severe xerostomia after treatment.⁸

Most patients with NPC present with moderate-to-advanced stage disease at initial diagnosis, with the tumour usually extending outside the nasopharyngeal region. Over 60% of them involve the PPS⁹ and/or level IIa cervical lymph nodes,¹⁰ which are in close proximity to the deep lobe of the parotid gland. Therefore, it is likely that

relatively high doses would be delivered to the parotid in radiotherapy. Deasy et al¹¹ reported that severe radiation-induced xerostomia could be avoided if both entire parotid glands were kept to a mean dose of below 25 Gy, which poses a challenge to the dosimetrists for computing treatment plans for these patients.

Recently, it has been reported that the recovery of a salivary gland injury after radiation therapy was dependent on the radiation dose and amount of residual dynamic stem cell in the salivary gland pre-clinically.¹² Therefore, the reduction of dose in parotid gland stem cells might promote its recovery in patients. Pre-clinical studies on mice revealed that restricting the dose to this region of the gland produced more rapid recovery of gland function after irradiation.^{13,14} Since with reference to the mice model, the stem cells of the salivary gland were detected at the main excretory ducts,^{15,16} which are mainly located at the anterolateral subsegment of the parotid gland,¹⁷ in order to better protect the stem cells in the parotid gland during radiotherapy, a “split-parotid delineation” approach would be useful in which an imaginary line is drawn through the anterolateral margin of the retromandibular vein, which divides the parotid gland into the anterolateral and posteromedial subsegments (Figure 1). By applying a more stringent dose constraint to the anterolateral subsegment, which is where the stem cells are mainly located, there might be a better chance to preserve the function of the parotid gland.

The aim of this study was to evaluate the dosimetric impact of applying the split-parotid delineation method in volumetric-modulated radiotherapy (VMAT) of patients with NPC with PPS and/or level IIa cervical node involvements and how it

Figure 1. A transverse CT image showing the parotid gland contours being split into anterolateral and posteromedial subsegments. It is expected that most stem cells will be located at the anterolateral subsegment of the parotid gland.



might reduce the risk of xerostomia in patients by better sparing the putative stem cell niche in the parotid gland.

METHODS AND MATERIALS

50 newly diagnosed patients with NPC treated with VMAT between February 2012 and June 2014 were recruited from the Cancer Hospital, Shantou University Medical College. The patient characteristics are shown in Table 1. They were divided into three groups according to the location of the tumour extension. Group 1 consisted of patients with level IIa cervical lymph node metastases only ($n = 15$); Group 2 was patients with unilateral PPS invasion only ($n = 15$); and Group 3 consisted of patients who had both unilateral PPS and level IIa cervical lymph node involvements ($n = 20$).

All patients underwent planning CT scan in a supine treatment position and were immobilized with custom thermoplastic immobilization devices. The scan covered from the vertex to the upper mediastinum with a slice thickness of 3 mm. A VMAT plan was computed for each patient with the Eclipse treatment-planning system (Varian® Medical Systems, Palo Alto, CA) with 6 MV using a TrueBeam linear accelerator (Varian Medical

Table 1. Clinical characteristic of the patients with nasopharyngeal carcinoma in different patient groups

Characteristic	Group 1 ($n = 15$)	Group 2 ($n = 15$)	Group 3 ($n = 20$)
Sex			
Male	11 (73.33%)	9 (60.00%)	12 (60.00%)
Female	4 (26.67%)	6 (40.00%)	8 (40.00%)
Age (years)			
<60	10 (66.67%)	11 (73.33%)	14 (70.00%)
≥60	5 (33.33%)	4 (26.67%)	6 (30.00%)
T stage			
T1	5 (33.33%)	0 (0%)	0 (0%)
T2	8 (53.33%)	4 (26.67%)	5 (25.00%)
T3	2 (13.34%)	7 (46.66%)	10 (50.00%)
T4	0 (0%)	4 (26.67%)	5 (25.00%)
N stage			
N0	0 (0%)	1 (6.67%)	0 (0%)
N1	5 (33.33%)	6 (40.00%)	1 (5.00%)
N2	10 (66.67%)	8 (53.33%)	14 (70.00%)
N3	0 (0%)	0 (0%)	5 (25.00%)
Clinical stage			
I	0 (0%)	0 (0%)	0 (0%)
II	4 (26.67%)	2 (13.33%)	0 (0%)
III	11 (73.33%)	9 (60.00%)	10 (50.00%)
IVa	0 (0%)	4 (26.67%)	5 (25.00%)
IVb	0 (0%)	0 (0%)	5 (25.00%)

Systems). The target volumes were delineated according to the International Commission on Radiation Units and Measurements reports 50 and 62 guidelines.^{18,19} Image registration with MRI of the patient was performed to provide a delineation reference for the targets. Gross tumour volume was defined as the gross extent of the tumour shown by CT/MRI images, and this included the gross tumour at nasopharynx (GTVnx) and regional lymph nodes (GTVnd). Planning target volume at nasopharynx (PTVnx) and lymph node (PTVnd) were generated by adding 5–10 mm to the GTVnx and GTVnd, respectively. In addition, the high-risk regions outside the PTVnx and PTVnd that included the entire nasopharyngeal mucosa plus 5 mm into the submucosal, and the high-risk lymphatic drainage area was delineated as clinical target volume 1 (CTV1). By adding a 5-mm margin to the CTV1, the planning target volume 1 (PTV1) was created. In this study, only the parotid gland that was situated at the same side (ipsilateral side) of the PPS and/or level II nodes were evaluated in detail. The organs at risk (OARs), apart from the ipsilateral parotid gland, including the contralateral parotid gland, spinal cord, brain stem, ipsilateral temporomandibular joint, oral cavity, thyroid and larynx, were also contoured. The prescriptions for all patients were to give 70 Gy to PTVnx; 66 Gy to PTVnd; and 60 Gy to PTV1 in 30 fractions using a simultaneous integrated boost. For each VMAT plan, the collimator rotation was set at 30° and two coplanar arcs were delivered in opposite gantry rotation directions (clockwise and anticlockwise). All patients were treated with a 6-MV photon using TrueBeam linear accelerator (Varian Medical System). The planning objectives for the target volumes and OARs were set with reference to Radiation Therapy Oncology Group 0615 recommendations (Table 2). The treatment plan generated was

Table 2. The optimization objectives of the control and test plans for patients with nasopharyngeal carcinoma patients

Structures	Optimization objectives
PTVnx	$V_{100} \geq 95\%$, $D_1 \leq 77$ Gy
PTVnd	$V_{100} \geq 95\%$
PTV1	$V_{100} \geq 95\%$
Brain stem	$D_1 < 60$ Gy
Spinal cord	$D_1 < 45$ Gy
Optic nerve	$D_1 < 50$ Gy
Optic chiasm	$D_{\max} < 54$ Gy
Lens	$D_1 < 10$ Gy
Pituitary	$D_{\text{mean}} < 50$ Gy
Larynx	$D_{\text{mean}} < 40$ Gy
TM joint	$D_{\text{mean}} < 50$ Gy
Oral cavity	$D_{\text{mean}} < 40$ Gy
Parotid gland	$D_{\text{mean}} < 35$ Gy
Thyroid gland	$D_{\text{mean}} < 50$ Gy

D_1 , dose received by 1% volume; D_{\max} , maximum dose; D_{mean} , mean dose; PTV1, planning target volume 1; PTVnd, planning target volume of lymph nodes; PTVnx, planning target volume at nasopharynx; TM, temporomandibular; V_{100} , percentage of the volume that received 100% of the prescribed dose.

labelled as the “control plan”, in which the parotid gland was contoured as a single OAR to which the routine dose constraint was applied. A second plan, named the “test plan” in this study, was then computed for each patient using the same set of CT data and contoured structures. In this plan, a line through the anterolateral margin of the retromandibular vein was created that divided the parotid gland into the anterolateral and posteromedial subsegments (Figure 1). A mean dose constraint of 25 Gy was applied to the anterolateral subsegment before the optimization, with the same dose requirements for the target volumes and other OARs as the control plan.

The dosimetric data of each treatment plan were collected and recorded through the generation of dose–volume histograms. The evaluated dose parameters for the parotid gland were V_{15} , V_{20} , V_{25} , V_{30} and V_{35} (volume of organ receiving 15, 20, 25, 30 and 35 Gy, respectively) and D_{mean} (mean dose). For the PTV1, the D_{\max} (maximum dose), D_{mean} , conformity index (CI) and homogeneity index (HI) were included as the assessment parameters. CI was calculated using the equation: $CI = (PTV_{\text{ref}} \div V_{\text{PTV}}) \times (PTV_{\text{ref}} \div V_{\text{ref}})$,²⁰ where PTV_{ref} represents the volume receiving the prescribed dose in the target volume; V_{PTV} was the volume of the planning target volume (PTV) and V_{ref} was the volume that received the prescribed dose. HI was calculated as the difference between D_1 and D_{99} divided by the prescribed dose,^{21,22} where D_{99} and D_1 represent the dose received by 99% and 1% of the volume, respectively. For the OARs, D_1 (Dose received by 1% volume of the organ) was used to evaluate the doses to the brain stem, spinal cord, optic nerves and lens, and D_{mean} was used to evaluate the doses to the pituitary, ipsilateral temporomandibular joints, contralateral parotid glands, oral cavity, thyroid and larynx. D_{\max} was used to evaluate the doses to the optic chiasm. A summary of all the dose parameters for the targets, parotid gland and the various OARs are listed in Supplementary Table A. For each of the three patient groups, the mean of each dose parameter was compared between the control plan and test plan. SPSS® v. 20.0 (IBM Corp., New York, NY; formerly SPSS Inc., Chicago, IL) was applied for statistical analysis. Paired *t*-test or Wilcoxon test was conducted depending on the normality of the data to evaluate the differences between the two types of plans for each patient group.

RESULTS

Dose to the ipsilateral parotid gland

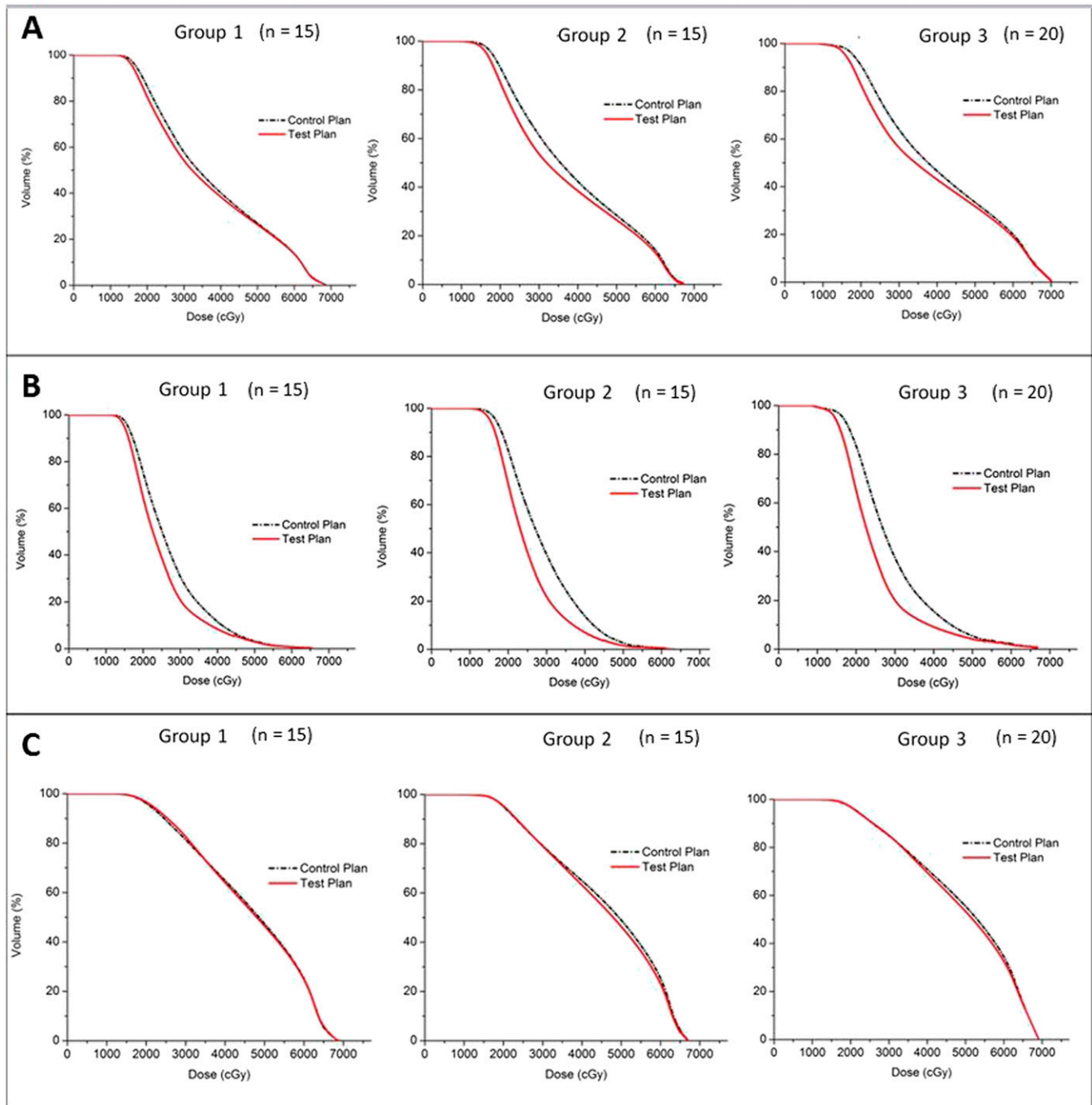
With regard to the entire parotid gland, the mean doses in all treatment plans were above 36 Gy and they increased from Group 1 to Group 3. The differences of their means were significant (analysis of variance, $p < 0.001$), in which Group 2 was significantly greater than Group 1 (Tukey’s test, $p = 0.004$), and Group 3 was significantly greater than Group 2 (Tukey test, $p = 0.006$). All the dose parameters of the test plans were significantly lower than that of the control plans in all the three patient groups (Table 3, Figure 2). The mean doses of the anterolateral subsegment in all the three groups were all less than 25 Gy, and they also increased from Group 1 to Group 3. Besides, all the dose parameters of the test plans were significantly lower than that of the control plans. For the posteromedial subsegment, its mean doses were in general higher than those in the anterolateral subsegment. Most of the dose parameters between the control and test plan did not show

Table 3. Comparisons of doses to the ipsilateral parotid gland between the control and test plans in the three different patient groups

Dose-volume parameters	Group 1 (n = 15)			Group 2 (n = 15)			Group 3 (n = 20)		
	Control plan (mean ± SD)	Test plan (mean ± SD)	p-value	Control plan (mean ± SD)	Test plan (mean ± SD)	p-value	Control plan (mean ± SD)	Test plan (mean ± SD)	p-value
Whole gland									
D_{mean} (Gy)	37.50 ± 2.30	36.42 ± 2.04	0.001	38.45 ± 4.00	36.44 ± 3.45	0.000	40.55 ± 2.85	38.45 ± 2.77	0.000
V_{15} (%)	98.53 ± 1.66	97.29 ± 2.49	0.001	98.93 ± 1.84	97.74 ± 2.56	0.001	98.56 ± 4.56	96.80 ± 4.94	0.000
V_{20} (%)	86.33 ± 7.10	81.55 ± 5.98	0.000	89.23 ± 6.99	83.08 ± 6.59	0.000	90.78 ± 7.95	82.69 ± 7.69	0.000
V_{25} (%)	71.08 ± 7.06	66.20 ± 5.01	0.000	74.00 ± 9.95	66.18 ± 8.52	0.000	76.39 ± 8.55	67.39 ± 5.84	0.000
V_{30} (%)	57.81 ± 6.36	53.94 ± 4.90	0.000	61.35 ± 11.25	53.65 ± 8.92	0.001	63.93 ± 7.90	56.35 ± 6.22	0.000
V_{35} (%)	48.09 ± 6.23	45.44 ± 4.95	0.001	50.98 ± 10.83	45.26 ± 8.88	0.001	54.20 ± 7.91	49.10 ± 6.93	0.000
Anterolateral subsegment									
D_{mean} (Gy)	27.30 ± 1.58	24.98 ± 0.73	0.001	28.82 ± 2.74	25.07 ± 0.78	0.001	29.26 ± 1.65	25.15 ± 0.41	0.000
V_{15} (%)	97.45 ± 3.03	94.79 ± 4.89	0.001	98.28 ± 3.07	95.72 ± 5.05	0.001	97.40 ± 8.14	93.50 ± 9.17	0.000
V_{20} (%)	75.32 ± 11.60	64.17 ± 10.00	0.000	82.47 ± 9.31	68.46 ± 9.22	0.000	83.40 ± 13.09	65.10 ± 12.85	0.000
V_{25} (%)	50.42 ± 10.64	38.35 ± 6.32	0.001	58.32 ± 12.44	40.25 ± 5.95	0.001	57.98 ± 12.07	37.67 ± 5.46	0.000
V_{30} (%)	30.83 ± 8.64	20.72 ± 5.05	0.001	39.23 ± 13.68	21.85 ± 3.10	0.001	37.47 ± 8.93	20.13 ± 5.36	0.000
V_{35} (%)	19.20 ± 6.62	13.30 ± 4.19	0.000	24.60 ± 12.07	12.55 ± 3.76	0.001	23.92 ± 7.35	13.07 ± 5.04	0.000
Posteromedial subsegment									
D_{mean} (Gy)	46.33 ± 2.86	46.24 ± 2.76	0.597	46.15 ± 5.21	45.51 ± 5.00	0.042	49.44 ± 4.13	48.94 ± 4.11	0.005
V_{15} (%)	99.60 ± 0.90	99.59 ± 0.90	0.600	99.54 ± 1.09	99.54 ± 1.22	0.917	99.64 ± 1.32	99.69 ± 1.15	0.612
V_{20} (%)	96.12 ± 4.30	96.41 ± 4.23	0.140	95.10 ± 6.40	95.32 ± 5.96	0.496	96.85 ± 3.97	96.85 ± 3.71	0.570
V_{25} (%)	89.29 ± 6.27	90.09 ± 6.06	0.022	87.02 ± 10.40	87.20 ± 10.43	0.910	90.92 ± 7.63	91.01 ± 7.36	0.723
V_{30} (%)	81.35 ± 7.21	82.40 ± 6.57	0.091	79.21 ± 12.76	79.02 ± 12.78	0.722	85.01 ± 10.04	85.06 ± 9.45	1.000
V_{35} (%)	73.14 ± 7.04	72.99 ± 5.89	0.838	71.92 ± 13.50	71.09 ± 13.62	0.092	78.12 ± 10.55	77.51 ± 9.87	0.108

 D_{mean} , mean dose; SD, standard deviation.

Figure 2. Comparison of dose–volume histograms between the control plan and test plan in the three different patient groups (1–3) for the (a) whole ipsilateral parotid gland, (b) anterolateral subsegment and (c) posteromedial subsegment of the ipsilateral parotid gland.



significant difference, except for the D_{mean} of Groups 2 and 3 and V_{25} of Group 1.

Dose to targets and organs at risk

All the targets met the dose requirements set for plan optimization. For the doses to the PTVs, the dosimetric differences between the control and test plans were small ($<1\%$), with only a few differences in Group 1 and 3 reaching statistical significance (Table 4). For the doses to the OARs, all of them received

doses within their dose limits. Apart from the contralateral parotid gland and oral cavity, there was no significant difference between the control and test plans for the rest of the OARs in all the three groups (Table 5).

DISCUSSION

The application of the split-organ delineation approach to the parotid gland in treatment planning had been used in some previous studies. Chau et al²³ had reported splitting the organs

Table 4. Comparisons of doses to the target between the control and test plans in different patient groups

Dose-volume parameters	Group 1 (n = 15)			Group 2 (n = 15)			Group 3 (n = 20)		
	Control plan (mean ± SD)	Test plan (mean ± SD)	p-value	Control plan (mean ± SD)	Test plan (mean ± SD)	p-value	Control plan (mean ± SD)	Test plan (mean ± SD)	p-value
PTVnx									
V ₁₀₀ (%)	96.47 ± 1.79	95.91 ± 1.73	0.024	95.89 ± 1.51	95.70 ± 1.56	0.267	95.71 ± 1.28	95.45 ± 1.14	0.825
V ₉₃ (%)	100.00 ± 0.00	100.00 ± 0.00	1.000	99.95 ± 0.13	99.96 ± 0.14	0.655	99.92 ± 0.23	99.93 ± 0.20	0.109
D _{mean} (Gy)	71.71 ± 0.54	71.66 ± 0.61	0.609	71.82 ± 0.51	71.85 ± 0.68	0.910	72.04 ± 0.48	72.11 ± 0.42	0.232
PTVnd									
V ₁₀₀ (%)	98.15 ± 1.75	98.04 ± 1.95	0.666	97.45 ± 2.07	97.32 ± 1.73	0.690	97.21 ± 2.02	97.29 ± 2.22	0.825
V ₉₃ (%)	100.00 ± 0.00	100.00 ± 0.00	1.000	99.81 ± 0.60	99.80 ± 0.63	1.000	99.87 ± 0.27	99.85 ± 0.30	0.024
D _{mean} (Gy)	68.61 ± 1.34	68.66 ± 1.40	0.784	68.41 ± 1.07	68.58 ± 1.56	0.790	69.08 ± 1.19	69.29 ± 1.31	0.027
PTV1									
V ₁₀₀ (%)	95.06 ± 1.02	95.62 ± 0.84	0.016	95.48 ± 1.07	95.71 ± 0.87	0.184	94.81 ± 1.25	95.23 ± 1.36	0.015
V ₉₃ (%)	99.90 ± 0.21	99.92 ± 0.18	0.192	99.84 ± 0.29	99.82 ± 0.32	0.859	99.52 ± 0.55	99.50 ± 0.57	0.568
D _{mean} (Gy)	64.60 ± 1.04	64.66 ± 1.11	0.427	65.08 ± 0.91	65.10 ± 1.01	0.865	65.99 ± 0.93	66.12 ± 0.94	0.030
D _{max} (Gy)	74.54 ± 0.91	74.46 ± 1.01	0.766	74.54 ± 0.80	74.61 ± 1.14	0.688	75.09 ± 0.55	75.33 ± 0.61	0.029
CI	0.87 ± 0.03	0.87 ± 0.03	1.000	0.86 ± 0.04	0.86 ± 0.04	1.000	0.87 ± 0.02	0.87 ± 0.02	1.000
HI	0.05 ± 0.01	0.05 ± 0.01	0.880	0.06 ± 0.02	0.06 ± 0.02	0.609	0.07 ± 0.02	0.08 ± 0.02	0.017

CI, conformity index; D_{max}, maximum dose; D_{mean}, mean dose; HI, homogeneity index; PTV1, planning target volume 1; PTVnd, planning target volume of lymph nodes; PTVnx, planning target volume at nasopharynx; SD, standard deviation.

Table 5. Comparisons of doses to the organs at risk between the control and test plans in different patient groups

Dose parameters	Group 1 (n = 15)			Group 2 (n = 15)			Group 3 (n = 20)		
	Control plan (mean ± SD)	Test plan (mean ± SD)	p-value	Control plan (mean ± SD)	Test plan (mean ± SD)	p-value	Control plan (mean ± SD)	Test plan (mean ± SD)	p-value
Contra parotid gland D_{mean} (Gy)	36.65 ± 2.32	35.85 ± 2.07	0.040	38.18 ± 3.00	36.49 ± 2.70	0.010	39.15 ± 2.07	37.70 ± 2.31	0.010
Brain stem D_1 (Gy)	45.10 ± 3.02	45.06 ± 3.04	0.765	47.16 ± 3.91	47.07 ± 4.00	0.458	48.66 ± 5.13	48.35 ± 5.49	0.344
Spinal cord D_1 (Gy)	39.21 ± 1.46	39.27 ± 1.45	0.865	38.77 ± 1.48	38.94 ± 1.50	0.190	39.98 ± 1.87	40.22 ± 1.84	0.141
Ipsi TM joint D_{mean} (Gy)	33.35 ± 4.45	33.46 ± 4.25	0.663	35.27 ± 6.22	34.60 ± 6.20	0.090	38.06 ± 9.67	37.92 ± 9.91	0.550
Oral cavity D_{mean} (Gy)	35.91 ± 2.07	35.89 ± 3.21	0.012	37.24 ± 2.62	37.83 ± 2.65	0.001	36.50 ± 2.98	37.24 ± 3.28	0.001
Larynx D_{mean} (Gy)	38.60 ± 2.36	38.75 ± 2.25	0.271	37.77 ± 3.30	37.56 ± 3.29	0.075	38.76 ± 2.02	38.59 ± 2.28	0.341
Thyroid D_{mean} (Gy)	42.09 ± 7.83	42.13 ± 7.89	0.754	38.73 ± 10.18	38.82 ± 10.17	0.201	45.43 ± 4.76	45.48 ± 4.82	0.615

Contra, contralateral; D_1 , dose received by 1% volume of the organ; D_{mean} , mean dose; ipsi, ipsilateral; SD, standard deviation; TM, temporomandibular.

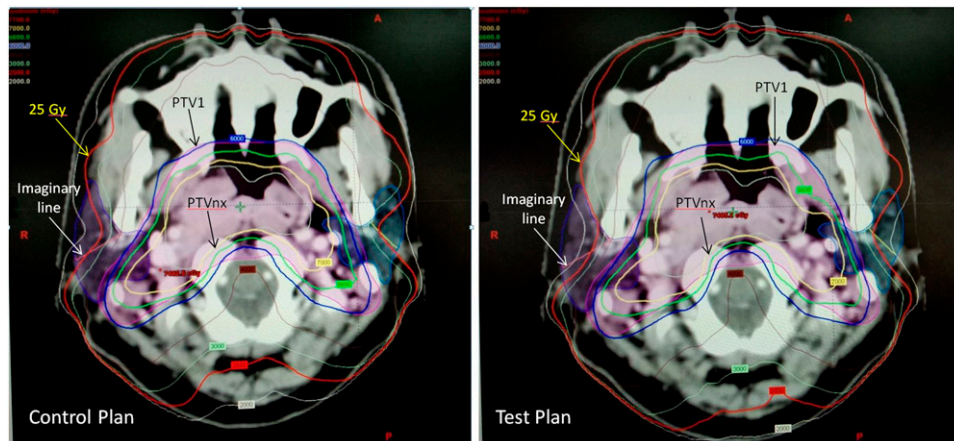
into target-overlapping and non-target-overlapping subsegments in contouring the parotid gland, while Zhang et al²⁴ reported splitting of the parotid glands into superficial and deep lobes. Shao et al¹⁷ studied the influence of a similar parotid-split delineation approach on patients with NPC with bilateral cervical nodes. Our study employed the split-parotid delineation method in the VMAT planning of patients with NPC to spare the stem cells of the parotid gland, which are thought to be concentrated at the anterolateral segment of the gland. The uniqueness of this study was that it focused on patients with NPC with PPS invasion and level IIa cervical lymph node metastases, which were anatomically close to the parotid gland.

By applying the split-parotid delineation approach and with a more stringent dose constraint to the anterolateral subsegment, our study demonstrated that this could lower the mean dose of the parotid gland and limit the mean dose of the anterolateral subsegment below 25 Gy without greatly compromising the doses to the target volumes and OARs. The dosimetric effect is illustrated in Figure 3, in which the 25 Gy isodose curve was pushed away from the anterolateral subsegment of the parotid gland in the test plan. Comparatively, the impact on PTV dose was the greatest in Group 3 than in the other two groups, where the D_{mean} , D_{max} and HI of this group showed significant differences. The explanation for this was because the PTVs in Group 3 with both PPS and level IIa nodal involvements were expected to be larger and closer to the parotid gland. The magnitude of dose reduction in the PTV would then be relatively more obvious when the dose to the anterolateral subsegment is reduced by applying the dose constraint. For the OARs, the doses to the oral cavity showed difference between the control and test plans. This could be owing to the fact that the oral cavity was the OAR that was located close to the parotid gland, and it was more affected by the change in the parotid dose. Nevertheless, the absolute differences in these parameters in both PTV and OARs were small; it was expected that they would not have significant clinical impact on the patients. For the contralateral parotid gland, since similar dose constraint as for the ipsilateral gland was applied in the test plan, its mean dose was lower than that of the control plan, although the differences were not as great as the ipsilateral side.

In addition, the mean dose of the anterolateral subsegment of the parotid gland demonstrated a significant increase from Group 1 to Group 3. This indicated that the influence of PPS invasion was greater than that of the level IIa cervical node involvement, whereas when both PPS invasion and level IIa cervical node involvement existed together, the dose impact to the anterolateral subsegment was the greatest.

At present, there is little knowledge about the dose limit of the stem cell in the parotid gland; it was logical to take the mean dose of 25 Gy suggested by Deasy et al¹¹ as the reference in this study because it has been the most conservative dose limit for the parotid gland of all previous related studies. The success in keeping the anterolateral subsegment below this dose level would be expected to help preserve the parotid gland function and reduce the risk of xerostomia, because this is the location where most of the parotid gland stem cells are thought to be

Figure 3. Comparison of the isodose distribution of a volumetric-modulated radiotherapy plan between the control plan and test plan for a patient with nasopharyngeal carcinoma in Group 3.



located. This effect was relatively more obvious in Group 3 than in Group 1, indicating that this split-parotid delineation approach offered greater benefit for patients with both PPS and level IIa cervical node involvements. It was because for patients in Group 3, the PTVs were more close to the parotid gland that caused a relatively higher mean dose to the anterolateral region of the gland in the control plan. Therefore, a greater dose reduction would be observed for this group when the dose of this subsegment is pushed below 25 Gy in the test plan. On the other hand, it was logical to see such dose difference effect did not exist in the posteromedial subsegment for all the three groups because no stringent dose constraint was applied to this region. With the positive results obtained from this study, it was expected that the application of this split-parotid delineation approach could be extended to other head and neck cases with the irradiation fields involving the parotid gland, so that the function of the gland could

be better preserved after radiotherapy. However, clinical validations of this planning approach followed by larger scale randomized clinical studies are required to evaluate the clinical outcomes.

CONCLUSION

The split-parotid delineation approach significantly lowered the mean dose to the anterolateral subsegment of the parotid gland and the overall gland in the VMAT of patients with NPC with PPS and/or level IIa cervical node involvements, without greatly compromising the doses to the target volumes and OARs. The effect was more obvious for both PPS and level IIa cervical node involvements (Group 3) than for either of them alone (groups 1 and 2). It was expected that such an approach could be extended to other head and neck cancers when irradiation fields involve the parotid gland so as to achieve better preservation of the gland function after radiotherapy.

REFERENCES

- Abendstein H, Nordgren M, Boysen M, Jannert M, Silander E, Ahlner-Elmqvist M, et al. Quality of life and head and neck cancer: a 5 year prospective study. *Laryngoscope* 2005; **115**: 2183–92. doi: <http://dx.doi.org/10.1097/01.MLG.0000181507.69620.14>
- Hammerlid E, Taft C. Health-related quality of life in long-term head and neck cancer survivors: a comparison with general population norms. *Br J Cancer* 2001; **84**: 149–56. doi: <http://dx.doi.org/10.1054/bjoc.2000.1576>
- Hammerlid E, Silander E, Hörnrestam L, Sullivan M. Health-related quality of life three years after diagnosis of head and neck cancer—a longitudinal study. *Head Neck* 2001; **23**: 113–25. doi: [http://dx.doi.org/10.1002/1097-0347\(200102\)23:2<113::AID-HED1006>3.0.CO;2-W](http://dx.doi.org/10.1002/1097-0347(200102)23:2<113::AID-HED1006>3.0.CO;2-W)
- Bjoridal K, Ahlner-Elmqvist M, Hammerlid E, Boysen M, Evensen JE, Bjorklund A, et al. A prospective study of quality of life in head and neck cancer patients. Part II: longitudinal data. *Laryngoscope* 2001; **111**: 1440–52. doi: <http://dx.doi.org/10.1097/00005537-200108000-00022>
- Bian X, Song T, Wu S. Outcomes of xerostomia-related quality of life for nasopharyngeal carcinoma treated by IMRT. *Expert Rev Anticancer Ther* 2015; **15**: 109–19. doi: <http://dx.doi.org/10.1586/14737140.2015.961427>
- Marucci L, Marzi S, Sperduti I, Giovannazzo G, Pinnarò P, Benassi M, et al. Influence of intensity-modulated radiation therapy technique on xerostomia and related quality of life in patients treated with intensity-modulated radiation therapy for nasopharyngeal cancer. *Head Neck* 2012; **34**: 328–35. doi: <http://dx.doi.org/10.1002/hed.21736>
- Kam MK, Leung SF, Zee B, Chau RM, Suen JJ, Mo F, et al. Prospective randomized study of intensity-modulated radiotherapy on salivary gland function in early-stagenasopharyngeal carcinoma patients. *J Clin Oncol* 2007; **25**: 4873–9.
- Vergeer MR, Doornaert PA, Rietveld DH, Leemans CR, Siotman BJ, Langendijk JA. Intensity modulated radiotherapy reduces radiation-induced morbidity and improves health related quality of life results of a non-randomized prospective study using a standardized follow-up program. *Int J Radiat Oncol Biol Phys* 2009; **74**: 1–8. doi: <http://dx.doi.org/10.1016/j.ijrobp.2008.07.059>
- Yu ZH, Xu GZ, Huang YR, Hu YH, Su XG, Gu XZ. Value of computed tomography in staging the primary lesion (T-staging) of nasopharyngeal carcinoma (NPC): an analysis of 54 patients with special reference to the

- parapharyngeal space. *Int J Radiat Oncol Biol Phys* 1985; **11**: 2143–7. doi: [http://dx.doi.org/10.1016/0360-3016\(85\)90095-1](http://dx.doi.org/10.1016/0360-3016(85)90095-1)
10. Wang X, Li L, Hu C, Zhou Z, Ying H, Ding J, et al. Patterns of level II node metastasis in nasopharyngeal carcinoma. *Radiother Oncol* 2008; **89**: 28–32. doi: <http://dx.doi.org/10.1016/j.radonc.2008.07.014>
 11. Deasy JO, Moiseenko V, Marks L, Chao KS, Nam J, Eisbruch A. Radiotherapy dose-volume effects on salivary gland function. *Int J Radiat Oncol Biol Phys* 2010; **76**: 58–63. doi: <http://dx.doi.org/10.1016/j.ijrobp.2009.06.090>
 12. Lombaert IM, Brunsting JF, Wierenga PK, Kampinga HH, de Haan G, Coppes RP. Keratinocyte growth factor prevents radiation damage to salivary glands by expansion of the stem/progenitor pool. *Stem Cells* 2008; **26**: 2595–601. doi: <http://dx.doi.org/10.1634/stemcells.2007-1034>
 13. Konings AW, Cotteleer F, Faber H, van Luijk P, Meertens H, Coppes RP. Volume effects and region-dependent radiosensitivity of the parotid gland. *Int J Radiat Oncol Biol Phys* 2005; **62**: 1090–5. doi: <http://dx.doi.org/10.1016/j.ijrobp.2004.12.035>
 14. Konings AW, Faber H, Cotteleer F. Secondary radiation damage as the main cause for unexpected volume effects: a histopathologic study of the parotid gland. *Int J Radiat Oncol Biol Phys* 2006; **64**: 98–105. doi: <http://dx.doi.org/10.1016/j.ijrobp.2005.06.042>
 15. Coppes RP, Stokman MA. Stem cells and the repair of radiation-induced salivary gland damage. *Oral Dis* 2011; **17**: 143–53. doi: <http://dx.doi.org/10.1111/j.1601-0825.2010.01723.x>
 16. Feng J, van der Zwaag M, Stokman MA, van Os R, Coppes RP. Isolation and characterization of human salivary gland cells for stem cell transplantation to reduce radiation-induced hyposalivation. *Radiother Oncol* 2009; **92**: 466–71. doi: <http://dx.doi.org/10.1016/j.radonc.2009.06.023>
 17. Shao MH, Ke WT, Jia HJ. A split-parotid delineation approach for dose optimisation in intensity-modulated radiotherapy for nasopharyngeal carcinoma with bilateral neck lymph node metastasis in level II. *J Chin Oncol* 2014; **20**: 40–6.
 18. A. International Commission on Radiation Units and Measurements. *ICRU report 50. Prescribing, recording, and reporting photon beam therapy*. Bethesda, MD; ICRU; 1993.
 19. B. International Commission on Radiation Units and Measurements. *ICRU report 62. Prescribing, recording, and reporting photon beam therapy*. Bethesda, MD; ICRU; 1999.
 20. van't Riet A, Mak AC, Moerland MA. A conformation number to quantify the degree of conformality in brachytherapy and external beam irradiation: application to the prostate. *Int J Radiat Oncol Biol Phys* 1997; **37**: 731–6.
 21. Clivio A, Fogliata A, Franzetti-Pellanda A. Volumetric-modulated arc radiotherapy for carcinomas of the anal canal: A treatment planning comparison with fixed field IMRT. *Radiother Oncol* 2009; **92**: 118–24. doi: <http://dx.doi.org/10.1016/j.radonc.2008.12.020>
 22. Lin X, Sun T, Wang C, Yin Y, Liu T, Cehn J. Dosimetric comparison of fixed field intensity modulated radiation therapy and RapidArc volumetric modulated arc therapy in treatment of multiple intracranial metastases. *Chin J Radiother Med Protect* 2010; **30**: 585–9.
 23. Chau RM, Leung SF, Kam MK, Cheung KY, Kwan WH, Yu KH, et al. A split organ delineation approach for dose optimization for intensity modulated radiotherapy for advanced T stage nasopharyngeal carcinoma. *Clin Oncol (R Coll Radiol)* 2008; **20**: 134–41. doi: <http://dx.doi.org/10.1016/j.clon.2007.10.006>
 24. Zhang HB, Lu X, Huang SM, Wang L, Zhao C, Xia WX, et al. Superficial parotid lobe-sparing delineation approach: a better method of dose optimization to protect the parotid gland in intensity-modulated radiotherapy for nasopharyngeal carcinoma. *Curr Oncol* 2013; **20**: 577–84. doi: <http://dx.doi.org/10.3747/co.20.1485>